DATA ANALYTICS AND APPLIED MATHEMATICS (DAAM)
e-ISSN: 2773-4854
VOL. 3, ISSUE 1, 028 – 041
DOI: https://doi.org/10.15282/daam.v3i1.7594

ORIGINAL ARTICLE

Stability, cost-effectiveness, and global sensitivity analysis of COVID-19 model incorporating non-pharmaceutical interventions and indirect transmission

Darmawati[1*], W. Nur[1]

[1]Department of Mathematics, Universitas Sulawesi Barat, 91414 Majene, Indonesia

ABSTRACT – Covid-19 is an ongoing pandemic caused by SARS-CoV-2. Some interventions are implemented to control the spread of the disease. In Indonesia, there is a campaign related to non-pharmaceutical approach called 3M. This campaign is carried out so that people use masks, wash their hands, and keep their distance. In this paper, we propose a mathematical model considering non-pharmaceutical interventions and indirect transmission. The non-pharmaceutical interventions studied are the implementation of mask-wearing, handwashing, and social distancing. The model is presented as a system of first-order differential equations. The basic reproduction number is determined. The system has two equilibrium points, namely the disease-free equilibrium point and the endemic equilibrium point. The local stability condition of the disease-free equilibrium point is proved using the Lienard-Chipart criterion. Center manifold theory is used to prove the local stability condition of the endemic equilibrium point. We also study the optimal control strategy related to mask-wearing, handwashing, and social distancing. Furthermore, cost-effectiveness analysis of intervention strategies is also conducted by studying the average cost-effectiveness ratio of each intervention strategy. Our results show that the most effective strategy to control covid-19 spread is the combination of mask-wearing, handwashing, and social distancing. Moreover, the most cost-effective strategy is mask-wearing intervention. Global sensitivity analysis is performed by studying the partial rank correlation coefficient. The results show that mask-wearing intervention is the most influential intervention on basic reproduction number compared to social distancing and handwashing.

ARTICLE HISTORY
Received:04/01/2022
Revised: 03/03/2022
Accepted: 30/03/2022

KEYWORDS
Stability analysis
Optimal control
Cost-effectiveness
Global sensitivity
Covid-19

INTRODUCTION

Covid-19 is an ongoing pandemic which is caused by SARS-CoV-2 infection [1]. At the end of December 2019, Wuhan Health Commission reported the outbreak of unknown pneumonia [2]. However, the cases occur since December 8, 2019 in Wuhan, China [1]. It is stated that this disease is the third coronavirus crisis since 2002 [2]. SARS-CoV-2 belongs to the Coronaviridae family [3]. It is well known that coronavirus primarily targets human respiratory system [4]. SARS-CoV-2 is highly infectious and has spread to no less than 200 countries. This is the reason why WHO stated that covid-19 is a global threat (pandemic) [5].

In the beginning of the outbreak, it is believed that the transmission occurs from infected animal to human. However, it is now clear that the transmission occurs due to close contact or exposure to virus [3]. The transmission caused by sneezing, coughing, and sometimes talking is classified as direct transmission [6]. To reduce covid-19 spread, social distancing should be practiced [1], [5]. Ong et al. [7] and Wu et al. [8] stated that contaminated environment with infected person's droplet potentially becomes a medium of transmission. Based on this information, the transmission may occur even though there is no a direct interaction between infected person and uninfected person. Therefore, we can say that this transmission mechanism is indirect transmission. To reduce covid-19 transmission, some researchers have recomended that we should not touch our eyes, mouth, and nose with unwashed hand [5]. In addition, the infected individuals should cover their mouth and nose by using tissue or mask [3]

One of the covid-19 mathematical models proposed in the beginning of the outbreak is discussed in [9]. The authors investigate the impact of mask use in reducing covid-19 burden. Mathematical model related covid-19 are also discussed in [10]–[18]. Several models proposed in these papers do not take into account the indirect transmission. The impact of non-pharmaceutical aproach on the spread of covid-19 is discussed in [11], [12], [15], [18]. Some of these papers also present optimal control problem [11-14], [16], [18].

In this paper, we propose covid-19 model considering mask-wearing, handwashing, social distancing, direct and indirect transmission. The main objectives of this work are to investigate the impact of non-phartmaceutical interventions on the spred of covid-19 when direct and indirect transmission are considered. To further explore the impact of indirect transmission of covid-19 and the effectiveness of non-pharmaceutical interventions, in this article, we discuss a cost-effectiveness analysis and global sensitivity analysis. Cost-effectiveness analysis is carried out by calculating the average cost-effectiveness ratio (ACER) of each intervention. The method given in [19] is used in performing the global sensitivity

*CORRESPONDING AUTHOR | Darmawati | ✉ darmath@unsulbar.ac.id

analysis.The paper is established as follows. The model construction is discussed in section 2. In section 3 and section 4, we present the basic properties of our proposed model and the basic reproduction number obtained, respectively. Stability analysis is discussed in section 5. In section 6, we study the optimal control problem of proposed model. Numerical simulation results for optimal control problem, cost-effectiveness analysis, and global sensitivity analysis are presented in section 7.

MODEL CONSTRUCTION

In this section, we describe the model construction process. Firstly, we divide the human population into four compartments, namely susceptible human (S), latent human (L), infectious human (I), and recovered human (R). V represents SARS-CoV-2 on the surface of objects. The schematic diagram can be seen in Figure 1.

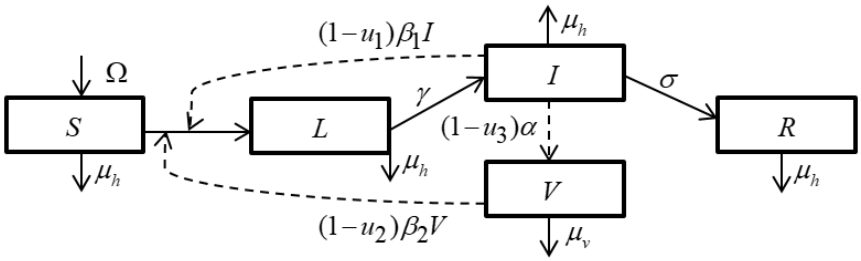

Figure 1. Schematic diagram.

The reduction in the number of susceptible humans happens due to direct and indirect transmission. We assume that direct transmission is affected by social distancing and indirect transmission is affected by handwashing. The dynamic of susceptible human compartment is represented by the following ordinary differential equation.

$$\frac{dS}{dt} = \Omega - (1-u_1)\beta_1 SI - (1-u_2)\beta_2 SV - \mu_h S,$$

where Ω is recruitment rate of susceptible humans, u_1 is proportion of susceptible humans who implement social distancing, u_2 is proportion of susceptible humans who impelement handwashing, β_1 is transmission rate from infectious humans to susceptible humans, β_2 is infection rate of viruses, and μ_h is the natural death rate of human. Susceptible humans who are infected through direct transmission or indirect transmission become latent humans. After completing the latent period, the latent humans leave latent human compartment and move to infectious human compartment. Further, latent humans are also reduced due to natural death. The dynamics of laten human compartment is described by the following differential equation.

$$\frac{dL}{dt} = (1-u_1)\beta_1 SI + (1-u_2)\beta_2 SV - \gamma L - \mu_h L,$$

where is $\gamma = \dfrac{1}{\text{Latent period}}$. Infectious humans who have recovered leave the infectious human compartment and move to the recovered human compartment. Thus, the dynamic of infectious human compartment is represented by the following equation

$$\frac{dI}{dt} = \gamma L - \sigma I - \mu_h I,$$

where σ is recovery rate. The recovered human compartment dynamics is described by

$$\frac{dR}{dt} = \sigma I - \mu_h R.$$

The increase in the number of SARS-CoV-2 in the environtment occurs due to droplets released by infectious humans. Therefore, the amount of virus released by infectious humans is affected by the use of masks. Further, the amount of virus on the surface of the object is reduced due to the natural death of the virus (μ_v). Therefore, the dynamics of SARS-CoV-2 on the surface of objects is represented by equation

$$\frac{dV}{dt} = (1-u_3)\alpha I - \mu_v V,$$

where u_3 is the proportion of infectious human who use mask and α is the average amount of SARS-CoV-2 released by one infectious person per day. Therefore, the model obtained from the model construction process above is expressed as

$$\begin{aligned}
\frac{dS}{dt} &= \Omega - (1-u_1)\beta_1 SI - (1-u_2)\beta_2 SV - \mu_h S,\\
\frac{dL}{dt} &= (1-u_1)\beta_1 SI + (1-u_2)\beta_2 SV - \gamma L - \mu_h L,\\
\frac{dI}{dt} &= \gamma L - \sigma I - \mu_h I,\\
\frac{dR}{dt} &= \sigma I - \mu_h R.\\
\frac{dV}{dt} &= (1-u_3)\alpha I - \mu_v V,
\end{aligned} \tag{1}$$

where $u_1, u_2, u_3 \in [0,1)$, $\Omega > 0$, and the other parameters are positive. We assume that the control parameter never reaches 1 because there are always groups of people who are ignorant of the appeal to use masks, wash hands, and keep a distance.

BASIC PROPERTIES AND EQUILIBRIUM POINTS

In this section, we present the basic properties and equilibrium points of system (1).

Theorem 1. *If initial values given are non-negative, then the solutions of system (1) are non-negative and bounded.*

Proof. Firstly, we show that the invariant region of system (1) is R^5_{+0}. From system (1), we get

$$\begin{aligned}
\left.\frac{dS}{dt}\right|_{S=0,L\geq 0,I\geq 0,R\geq 0,V\geq 0} &= \Omega > 0,\\
\left.\frac{dL}{dt}\right|_{S\geq 0,L=0,I\geq 0,R\geq 0,V\geq 0} &= (1-u_1)\beta_1 SI + (1-u_2)\beta_1 SV \geq 0,\\
\left.\frac{dI}{dt}\right|_{S\geq 0,L\geq 0,I=0,R\geq 0,V\geq 0} &= \gamma L \geq 0,\\
\left.\frac{dR}{dt}\right|_{S\geq 0,L\geq 0,I\geq 0,R=0,V\geq 0} &= \sigma I \geq 0.\\
\left.\frac{dV}{dt}\right|_{S\geq 0,L\geq 0,I\geq 0,R\geq 0,V=0} &= (1-u_3)\alpha I \geq 0.
\end{aligned}$$

Since $\frac{dx_i}{dt} \geq 0$ for $x_i = 0$ and $x_{j\neq i} \geq 0$ where $i, j = 1,2,3,4,5$, $x_1 = S$, $x_2 = L$, $x_3 = I$, $x_4 = R$, $x_5 = V$, based on Lemma 2 in [20], we conclude that R^5_{+0} is invariant set of system (1). It is indicated that the solutions of system (1) are in R^5_{+0} if initial conditions given are in R^5_{+0}. Hence, if initial values given are non-negative, then the solutions of system (1) are non-negative.

Now we prove that the solutions of system (1) are bounded if initial values given are non-negative. We already stated that human population is divided into four disjoint compartments, i.e. S, L, I, R. Hence, we get $N = S + L + I + R$, where N is the total number of human. From the first four equations of system (1), we have

$$\frac{dN}{dt} = \Omega - \mu_h N. \tag{2}$$

It clear that (2) is the first-order linear differential equation. After solving (2), we have $N(t) \leq \frac{\Omega}{\mu_h}$. This result implies that $I(t) \leq \frac{\Omega}{\mu_h}$. From the last equation of system (1), we have

$$\begin{aligned}\frac{dV}{dt} &= (1-u_3)\alpha I - \mu_v V \\ &\le (1-u_3)\alpha\frac{\Omega}{\mu_h} - \mu_v V.\end{aligned}$$

Based on Gronwall inequality, it is proved that V is bounded, i.e., $V(t) \le \frac{(1-u_3)\alpha\Omega}{\mu_h\mu_v V}$. The proof is completed. □

To determine the equilibrium points, we set the left hand side of system (1) equal to zero and determine the resulted system solutions. There are two equilibrium points of the system, i.e., disease-free equilibrium point $\Gamma_0 = (S^*, L^*, I^*, R^*, V^*) = \left(\Omega/\mu_h, 0, 0, 0, 0\right)$ and endemic equilibrium point $\Gamma_1 = (S^{**}, L^{**}, I^{**}, R^{**}, V^{**})$, where

$$\begin{aligned}S^{**} &= \frac{\Omega\gamma - (\gamma+\mu_h)(\sigma+\mu_h)I^{**}}{\mu_h\gamma}, \\ L^{**} &= \frac{(\sigma+\mu_h)I^{**}}{\gamma}, \\ I^{**} &= \frac{(R_e-1)\mu_h\mu_v(\gamma+\mu_h)(\sigma+\mu_h)}{(1-u_1)\beta_1(\gamma+\mu_h)(\sigma+\mu_h)+(1-u_2)\beta_2(1-u_3)\alpha(\gamma+\mu_h)(\sigma+\mu_h)}, \\ R^{**} &= \frac{\sigma I^{**}}{\mu_h}, \\ V^{**} &= \frac{(1-u_3)\alpha I^{**}}{\mu_v}, \\ R_e &= \frac{(1-u_1)\beta_1\Omega\gamma}{\mu_h(\gamma+\mu_h)(\sigma+\mu_h)} + \frac{(1-u_2)\beta_2(1-u_3)\alpha\Omega\gamma}{\mu_h\mu_v(\gamma+\mu_h)(\sigma+\mu_h)}.\end{aligned}$$

It is easy to see that Γ_0 always exists in R^5_{+0}. Furthermore, Γ_1 exists in R^5_{+0} if $R_e > 1$. In the next section we show that the existence condition of Γ_1 is totally dependent on the basic reproduction number.

BASIC REPRODUCTION NUMBER

The reproduction number is obtained using next generation matrix described in [21]. The infected compartments are L, I, V. Hence, we get the following next-generation matrix

$$FV^{-1} = \begin{pmatrix} \frac{(1-u_1)\beta_1\Omega}{\mu_h(\gamma+\mu_h)(\sigma+\mu_h)} + \frac{(1-u_2)\beta_2(1-u_3)\alpha\Omega\gamma}{\mu_h\mu_v(\gamma+\mu_h)(\sigma+\mu_h)} & \frac{(1-u_1)\beta_1\Omega\gamma}{\mu_h(\sigma+\mu_h)} + \frac{(1-u_2)\beta_2(1-u_3)\alpha\Omega}{\mu_h\mu_v(\sigma+\mu_h)} & \frac{(1-u_2)\beta_2\Omega}{\mu_h\mu_v} \\ 0 & 0 & 0 \\ 0 & 0 & 0 \end{pmatrix}.$$

The characteristic polynomial of FV^{-1} is

$$P(\lambda) = \lambda^2\left(\lambda - \left(\frac{(1-u_1)\beta_1\Omega\gamma}{\mu_h(\gamma+\mu_h)(\sigma+\mu_h)} + \frac{(1-u_2)\beta_2(1-u_3)\alpha\Omega\gamma}{\mu_h\mu_v(\gamma+\mu_h)(\sigma+\mu_h)}\right)\right).$$

Following [21], the reproduction number is given by

$$R_0 = R_0^a + R_0^b,$$

where

$$R_0^a = \frac{(1-u_1)\beta_1\Omega\gamma}{\mu_h(\gamma+\mu_h)(\sigma+\mu_h)}, \qquad R_0^b = \frac{(1-u_2)\beta_2(1-u_3)\alpha\Omega\gamma}{\mu_h\mu_v(\gamma+\mu_h)(\sigma+\mu_h)}.$$

Notice that the basic reproduction number consists of two terms. The first term $\left(R_0^a\right)$ relates to direct transmission by infectious humans while the second term $\left(R_0^b\right)$ relates to indirect transmission that occurs due to the presence of viruses on the surface of objects. The first term denotes the secondary case produced by an infectious human during his infectious period. Meanwhile, the second term represents the secondary case produced by the virus during its lifetime on the surface of the object. It is clear that $R_e = R_0$. Hence, Γ_1 exists in R_{+0}^5 if $R_0 > 1$.

STABILITY ANALYSIS

Theorem 2. *If $R_0 < 1$ then Γ_0 is locally asymptotically stable. If $R_0 = 1$ then one eigenvalue of Jacobian matrix of system (1) at Γ_0 is zero. If $R_0 > 1$ then Γ_0 is unstable.*

Proof. The Jacobian matrix of system (1) at Γ_0 is given by

$$J(\Gamma_0) = \begin{pmatrix} -\mu_h & 0 & -(1-u_1)\beta_1 S^* & 0 & -(1-u_2)\beta_2 S^* \\ 0 & -(\gamma+\mu_h) & (1-u_1)\beta_1 S^* & 0 & (1-u_2)\beta_2 S^* \\ 0 & \gamma & -(\sigma+\mu_h) & 0 & 0 \\ 0 & 0 & \sigma & -\mu_h & 0 \\ 0 & 0 & (1-u_3)\alpha & 0 & -\mu_v \end{pmatrix}.$$

The characteristic equation of $J(\Gamma_0)$ is

$$H(\lambda) = (\lambda+\mu_h)^2 H_1(\lambda),$$

where

$$\begin{aligned} H_1(\lambda) &= \lambda^3 + h_1\lambda^2 + h_2\lambda + h_3, \\ h_1 &= (\gamma+\mu_h)+(\sigma+\mu_h)+\mu_v, \\ h_2 &= (\gamma+\mu_h)(\sigma+\mu_h)\left(\mu_v + 1 - R_0^a\right), \\ h_3 &= \left(1-R_0\right)\mu_v(\gamma+\mu_h)(\sigma+\mu_h). \end{aligned}$$

Notice that $J(\Gamma_0)$ has two negative eigenvalues i.e. $\lambda_1 = \lambda_2 = -\mu_h$. Since $u_1, u_2, u_3 \in [0,1)$ and the other parameters are positive, it is clear that $R_0^a, R_0^b > 0$. Hence, $R_0 < 1$ implies $R_0^a, R_0^b < 1$. Thus, if $R_0 < 1$ then $h_1, h_2, h_3 > 0$. Obviously, if $R_0 > 1$ then there is a sign change in the sequence of $H_1(\lambda)$ coefficient. Hence, based on Descartes' sign rule [22], there is a positive eigenvalue if $R_0 > 1$. Thus, Γ_0 is unstable if $R_0 > 1$.

We observe that if $R_0 = 1$ then $h_3 = 0$. This result suggests that $J(\Gamma_0)$ has simple zero eigenvalue if $R_0 = 1$. Now, we use Lienard-Chipart criterion to prove the local stability condition of Γ_0. Based on Lienard-Chipart criterion [23], Γ_0 is locally asymptotically stable if $h_1 > 0, h_1h_2 - h_3 > 0, h_3 > 0$. Clearly, $h_1 > 0$. Moreover, if $R_0 < 1$ then $h_3 > 0$. We can show that $h_1h_2 - h_3 > 0$ that is

$$\begin{aligned} h_1h_2 - h_3 &= \left((\gamma+\mu_h)+(\sigma+\mu_h)\right)\left(\left(\mu_v + \left(1-R_0^a\right)\right)(\gamma+\mu_h)(\sigma+\mu_h)\right) \\ &\quad + {\mu_v}^2\left((\gamma+\mu_h)+(\sigma+\mu_h)\right) + (1-u_3)\alpha\gamma(1-u_2)\beta_2 S^*. \end{aligned}$$

Certainly, if $R_0 < 1$ then $h_1h_2 - h_3 > 0$. Therefore, based on Lienard-Chipart criterion [23], if $R_0 < 1$ then Γ_0 is locally asymptotically stable. □

Theorem 3. *The endemic equilibrium point Γ_1 is locally asymptotically stable if $R_0 > 1$.*

Proof. It has been shown that $J(\Gamma_0)$ has simple zero eigenvalue if $R_0 = 1$. Therefore, we can use the method proposed in [24] to prove that there is a positive equilibrium point which is locally asymptotically stable when $R_0 > 1$. Based on Theorem 2, $R_0 = 1$ is a critical point of stability of the disease-free equilibrium point because one of the eigenvalues of the Jacobian matrix of the system at Γ_0 is 0. Firstly, we choose β as bifurcation parameter. It is easy to show that critical point of β that is equivalent to $R_0 = 1$ is

$$\beta_1^* = \left(1-R_0^b\right)\frac{\left(\gamma+\mu_h\right)\left(\sigma+\mu_h\right)\mu_h}{\left(1-u_1\right)\Omega}.$$

It is easy to check that $J\left(\Gamma_0,\beta_1^*\right)$ has simple zero eigenvalue. Next, we determine the left eigenvector $\vec{v}$ and right eigenvector $\vec{w}$ of $J\left(\Gamma_0,\beta_1^*\right)$ corresponding to zero eigenvalue. We get

$$v_1 = 0, \qquad w_1 = -\frac{\left(\left(1-u_1\right)\beta_1^* S^* \mu_v + \left(1-u_2\right)\beta_2 S^*\left(1-u_3\right)\alpha\right)\gamma w_2}{\mu_h\mu_v\left(\sigma+\mu_h\right)},$$

$$v_2 = \frac{\gamma v_3}{\gamma+\mu_h}, \qquad w_2 = w_2,$$

$$v_3 = v_3, \qquad w_3 = \frac{\gamma w_2}{\sigma+\mu_h},$$

$$v_4 = 0, \qquad w_4 = \frac{\sigma\gamma w_2}{\mu_h\left(\sigma+\mu_h\right)},$$

$$v_5 = \frac{\left(1-u_2\right)\beta_2 S^*\gamma v_3}{\mu_v\left(\gamma+\mu_h\right)}, \qquad w_5 = \frac{\left(1-u_3\right)\alpha\gamma w_2}{\mu_v\left(\sigma+\mu_h\right)},$$

where v_3 is arbitrarily positive and w_2 is determined when $\vec{v}.\vec{w}=1$. It is straightforward to show that $w_2>0$. Before aplying theorem 4.1 in [24], we set $x_1=S, x_2=L, x_3=I, x_4=R, x_5=V$ and $\frac{dx_i}{dt}=f_i$ for $i=1,2,3,4,5$. Hence, we get

$$v_2 w_1 w_3 \frac{\partial^2 f_2\left(\Gamma_0,\beta_1^*\right)}{\partial x_1\partial x_3} = -\left(\frac{\gamma v_3}{\gamma+\mu_h}\right)\left(\frac{\left(\left(1-u_1\right)\beta_1^* S^*\mu_v + \left(1-u_2\right)\beta_2 S^*\left(1-u_3\right)\alpha\right)\gamma w_2}{\mu_h\mu_v\left(\sigma+\mu_h\right)}\right)\left(\frac{\gamma w_2}{\sigma+\mu_h}\right)\beta_1^* < 0,$$

$$v_2 w_3 w_2 \frac{\partial^2 f_2\left(\Gamma_0,\beta_1^*\right)}{\partial x_3\partial x_1} = -\left(\frac{\gamma v_3}{\gamma+\mu_h}\right)\left(\frac{\gamma w_2}{\sigma+\mu_h}\right)\left(\frac{\left(\left(1-u_1\right)\beta_1^* S^*\mu_v + \left(1-u_2\right)\beta_2 S^*\left(1-u_3\right)\alpha\right)\gamma w_2}{\mu_h\mu_v\left(\sigma+\mu_h\right)}\right)\beta_1^* < 0,$$

$$v_2 w_3 \frac{\partial^2 f_2\left(\Gamma_0,\beta_1^*\right)}{\partial x_3\partial\beta} = \left(\frac{\gamma v_3}{\gamma+\mu_h}\right)\left(\frac{\gamma w_2}{\sigma+\mu_h}\right)\frac{\Omega}{\mu_h} > 0.$$

These results imply

$$\begin{aligned} a = \sum_{k,i,j=1}^{5} v_k w_i w_j \frac{\partial^2 f_k\left(\Gamma_0,\beta_1^*\right)}{\partial x_i\partial x_j} &= -\left(\frac{\gamma v_3}{\gamma+\mu_h}\right)\left(\frac{\left(\left(1-u_1\right)\beta_1^* S^*\mu_v + \left(1-u_2\right)\beta_2 S^*\left(1-u_3\right)\alpha\right)\gamma w_2}{\mu_h\mu_v\left(\sigma+\mu_h\right)}\right)\left(\frac{\gamma w_2}{\sigma+\mu_h}\right)\beta_1^* \\ &\quad -\left(\frac{\gamma v_3}{\gamma+\mu_h}\right)\left(\frac{\gamma w_2}{\sigma+\mu_h}\right)\left(\frac{\left(\left(1-u_1\right)\beta_1^* S^*\mu_v + \left(1-u_2\right)\beta_2 S^*\left(1-u_3\right)\alpha\right)\gamma w_2}{\mu_h\mu_v\left(\sigma+\mu_h\right)}\right)\beta_1^* \\ &< 0, \end{aligned}$$

$$a = \sum_{k,i,j=1}^{5} v_k w_i \frac{\partial^2 f_k\left(\Gamma_0,\beta_1^*\right)}{\partial x_i\partial\beta} = \left(\frac{\gamma v_3}{\gamma+\mu_h}\right)\left(\frac{\gamma w_2}{\sigma+\mu_h}\right)\frac{\Omega}{\mu_h} > 0.$$

Based on Theorem 4.1 in [24], forward bifurcation occurs at $\beta^*{}_1$ which is equivalent to $R_0=1$. Therefore, it is proved that Γ_1 is locally asymptotically stable if $R_0>1$. □

OPTIMAL CONTROL PROBLEM AND COST-EFFECTIVENESS ANALYSIS

In this section, we study optimal control stategy with u_1, u_2, u_3 as the control parameters. Our optimal control model is system (1). Our objective is to minimize the number of linfected humans (latent human + infectious human) and the number of SARS-CoV-2 on the surface of objects. Furthermore, we also want to minimize the intervention cost related to mask-wearing, handwashing, and social distancing. Therefore, we choose the following objective function.

$$F\left(L,I,V,u_1,u_2,u_3\right)=\int_0^T G\,dt,$$

where $G=D_1L+D_2I+D_3V+D_4{u_1}^2+D_5{u_2}^2++D_6{u_3}^2$. D_1, D_2, and D_3 are balancing cost factor for handling latent human, infectious human, and SARS-CoV-2 on the sufrace of objects, respectively. Meanwhile, D_4, D_5, D_6 are costs of implementing control u_1, u_2, and u_3, respectively.

The hamiltonian function is given by

$$\begin{aligned}\mathrm{H}\left(S,L,I,R,V,u_1,u_2,u_3\right)&= G+k_1\frac{dS}{dt}k_2\frac{dL}{dt}k_3\frac{dI}{dt}k_4\frac{dR}{dt}k_5\frac{dV}{dt}\\&=D_1L+D_2I+D_3V+D_4{u_1}^2+D_5{u_2}^2++D_6{u_3}^2\\&\quad+k_1\left(\Omega-\left(1-u_1\right)\beta_1SI-\left(1-u_2\right)\beta_2SV-\mu_hS\right)\\&\quad+k_2\left(\left(1-u_1\right)\beta_1SI+\left(1-u_2\right)\beta_2SV-\gamma L-\mu_hL\right)\\&\quad+k_3\left(\gamma L-\sigma I-\mu_hI\right)\\&\quad+k_4\left(\sigma I-\mu_hR\right)\\&\quad+k_5\left(\left(1-u_3\right)\alpha I-\mu_vV\right).\end{aligned}$$

Thus, the control system is given by (1), while the adjoint system is as follows

$$\begin{aligned}\frac{dk_1}{dt}&=-\frac{\partial\mathrm{H}}{\partial S}=\left(k_1-k_2\right)\left(1-u_1\right)\beta_1I+\left(k_1-k_2\right)\left(1-u_2\right)\beta_2V+k_1\mu_h,\\\frac{dk_2}{dt}&=-\frac{\partial\mathrm{H}}{\partial L}=-D_1+k_2\left(\gamma+\mu_h\right)-k_3\gamma,\\\frac{dk_3}{dt}&=-\frac{\partial\mathrm{H}}{\partial I}=-D_2+k_1\left(1-u_1\right)\beta_1S-k_2\left(1-u_1\right)\beta_1S+k_3\left(\sigma+\mu_h\right)-k_5\left(1-u_3\right)\alpha,\\\frac{dk_4}{dt}&=-\frac{\partial\mathrm{H}}{\partial R}=k_4\mu_h,\\\frac{dk_5}{dt}&=-\frac{\partial\mathrm{H}}{\partial V}=-D_3+k_1\left(1-u_2\right)\beta_2S-k_2\left(1-u_2\right)\beta_2S+k_5\mu_v,\end{aligned}$$

where $k_i(T)=0$ for $i=1,2,3,4,5$. Suppose $u_j\in\left[0,u_j^{\max}\right]$ for $j=1,2,3$. Solving $\frac{\partial\mathrm{H}}{\partial u_j}=0$ gives the optimal value of control paramters as follows

$$\begin{aligned}u_1^*&=\min\left\{\max\left\{0,\frac{\left(k_2-k_1\right)\beta_1SI}{2D_4}\right\},u_1^{\max}\right\},\\u_2^*&=\min\left\{\max\left\{0,\frac{\left(k_2-k_1\right)\beta_2SV}{2D_5}\right\},u_2^{\max}\right\},\\u_3^*&=\min\left\{\max\left\{0,\frac{k_5\alpha I}{2D_6}\right\},u_3^{\max}\right\}.\end{aligned}$$

Following[25], in this article, we use $\bar{E}$ to measure the effectiveness of each intervention strategy.

$$\bar{E}=1-\int_0^T\left(\frac{\left(\tilde{L}(t)+\tilde{I}(t)\right)}{\left(L(t)+I(t)\right)}\right)dt, \tag{3}$$

where $\tilde{L}(t)$ and $\tilde{I}(t)$ represent the number of latent humans and the number of infectious humans at time t, respectively, when the intervention strategy is applied. On the other hand, $L(t)$ and $I(t)$ denote the number of latent humans and the number of infectious humans at time t, respectively, when no intervention is involved. Therefore,

$\left(L(t)+I(t)\right)-\left(\tilde{L}(t)+\tilde{I}(t)\right)$ is the number of infected humans that have been avoided because of the intervention. From

the objective function to be minimized, $D_4u_1^2 + D_5u_2^2 + +D_6u_3^2$ is the cost of the intervention. According to [26], average cost-effectiveness ratio of intervention can be determined using the following formula.

$$\text{ACER} = \frac{\text{Cost of intervention}}{\text{The number of infected human averted}} \tag{4}$$

Therefore, following [27], we use the following equation to measure the ACER of intervention.

$$\text{ACER} = \frac{\int_0^T \left(D_4u_1^2 + D_5u_2^2 + +D_6u_3^2\right)dt}{\int_0^T \left(L(t)+I(t)\right) - \left(\tilde{L}(t)+\tilde{I}(t)\right)dt}. \tag{5}$$

NUMERICAL SIMULATIONS

We perform some numerical simulations using the parameter values given in the Table 1. The initial conditions used are $S(0) = 10000, L(0) = 1000, I(0) = 500, R(0) = 0, V(0) = 100000$.

Table 1. Parameter values.

Symbol	Values	Unit	Source
Ω	$\frac{10^5}{70\times 365}$	$\text{person}\times\text{day}^{-1}$	Estimation
β_1	2.79×10^{-7}	$\text{person}^{-1}\times\text{day}^{-1}$	[28]
β_2	4.3×10^{-11}	$\text{virus}^{-1}\times\text{day}^{-1}$	[28]
μ_h	$\frac{1}{70\times 365}$	day^{-1}	Estimation
γ	$\frac{1}{2\times 7}$	day^{-1}	Estimation
σ	$\frac{1}{2\times 7}$	day^{-1}	Assumption
α	10000	$\text{virus}\times\text{human}^{-1}\times\text{day}^{-1}$	[29]
μ_v	$\frac{1}{5}$	day^{-1}	[28]

The first simulation is performed using $u_1 = u_2 = u_3 = 0.2$. The reproduction number obtained is $2.2364 > 1$. Further we get $L^{**} = 19.4297$ and $I^{**} = 19.4191$. Based on Theorem 2 and Theorem 3, the disease-free equilibrium point is unstable and the endemic equilibrium point is locally asymptotically stable. This result suggests that (L, I) tend to $(19.4297, 19.4191)$. The numerical simulation result is given in Figure 2(a). Notice that the solution curve of $L + I$ tend to positive value, i.e., 38.8487. Therefore, our theoretical and numerical simulation result are alike.

For the second simulation, we perform the simulation using $u_1 = u_2 = u_3 = 0.8$. The reproduction number obtained is $0.1983 < 1$. Based on Theorem 2, the disease-free equilibrium point is locally asymptotically stable. This result implies that (L, I) tend to $(0,0)$. Notice that the solution curve $L + I$ shown in Figure 2(b) tend to zero. Therefore, our theoretical and numerical simulation result are alike. These results imply that non pharmaceutical approach can be used to control the spread of covid-19. We should use medical mask, keep our distance and wash our hands regularly.

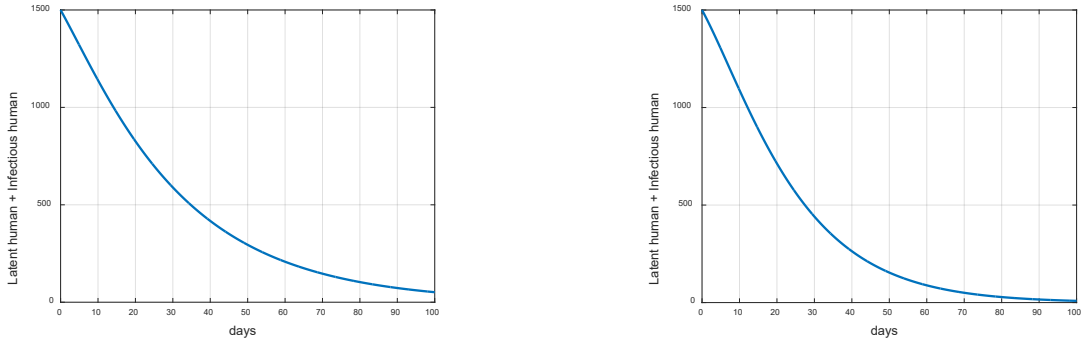

(a). $R_0 > 1$ **(b)** $R_0 < 1$

Figure 2. Dynamics of infected human when $R_0 > 1$ and $R_0 < 1$.

We now illustrate the forward bifurcation that occurs at β_1^*. By using the set of parameter value used in the second simulation, we obtain $\beta_1^* = 3.1453 \times 10^{-6}$. We set $\beta_1 \in \left[1.5726 \times 10^{-6}, 4.7180 \times 10^{-6}\right]$. The result can be seen in Figure 3. Clearly, when $\beta_1 < \beta_1^*$, I_h tend to zero which implies that Γ_0 is asymptotically stable . On the other hand, I_h converge to positive equilibrium which suggests that Γ_1 is asymptotically stable if $\beta_1 > \beta_1^*$. Furthermore, Γ_0 becomes unstable when $\beta_1 > \beta_1^*$.

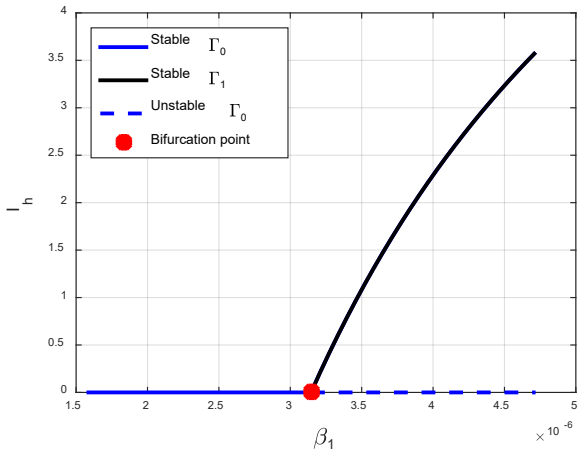

Figure 3. Forward bifurcation diagram of system (1) at β_1^* .

Global sensitivity analysis

A global sensitivity analysis is conducted using the method described in [19]. We generate latin hypercube sampling (LHS) matrix and determine partial rank correlation coefficient (PRCC) of each parameter. The number of simulations used is 20000. Figure 4 shows that parameter $\mu_h, \gamma, \sigma, \mu_v, u_1, u_2, u_3$ have negative relationtionship with basic reproduction number, while $\Omega, \beta_1, \beta_2, \alpha$ have positive relationship. Notice that σ is the parameter that has the most influence on R_0 among the parameters that have negative relationship. Furthermore, it is clear that among the control parameters, u_3 is the parameter that has the most influence on R_0 followed by u_2.

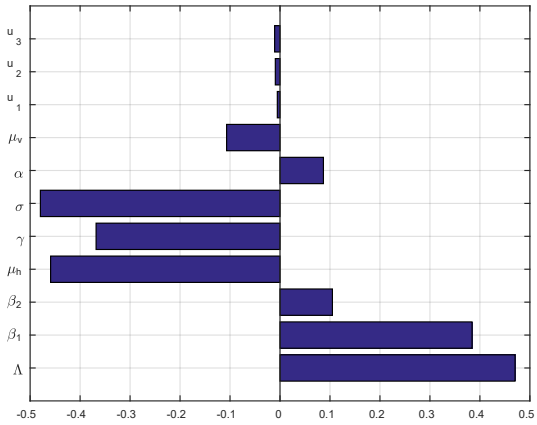

Figure 4. PRCC values when measured against basic reproduction number.

Optimal control and cost-effectiveness analysis

In this subsection, we present the numerical solution of optimal cotrol problem and cost effectiveness analysis. We investigate seven intervention schemes as follows

- Strategy 1: social distancing intervention only. In this strategy, we set $u_1 \geq 0, u_2 = 0, u_3 = 0$.
- Strategy 2: handwashing intervention only. In this strategy, we set $u_1 = 0, u_2 \geq 0, u_3 = 0$.
- Strategy 3: mask-wearing intervention only. In this strategy, we set $u_1 = 0, u_2 = 0, u_3 \geq 0$.
- Strategy 4: social distancing and handwashing intervention. In this strategy, we set $u_1 \geq 0, u_2 \geq 0, u_3 = 0$.
- Strategy 5: social distancing and mask-wearing intervention. In this strategy, we set $u_1 \geq 0, u_2 = 0, u_3 \geq 0$.
- Strategy 6: handwashing and mask-wearing intervention. In this strategy, we set $u_1 = 0, u_2 \geq 0, u_3 \geq 0$.
- Strategy 7: social distancing, handwashing, and mask-wearing intervention. In this strategy, we set $u_1 \geq 0, u_2 \geq 0, u_3 \geq 0$.

For the numerical simulations of optimal control problem, we choose $D_1 = 1, D_2 = 3, D_3 = 1, D_4 = 5, D_5 = 1, D_6 = 1$.

Strategy 1

The first simulation of the optimal control problem is performed to investigate the dynamics of the spread of covid-19 when there is an intervention, namely social distancing. Figures 5(a) and 5(b) show the dynamics of infected human and virus on the surface of object, respectively. As we can see, the difference between the solution curves of the model involving control and the model not involving control is not meaningful even though u_1 is at its maximum value as shown in Figure 5(c). When strategy 1 is applied, the number of infectious and latent humans on day 100 is 31 and 52, respectively. Meanwhile, the number of viruses is 3094869. It is smaller than the number of infectious humans, latent humans, and viruses when no intervention is practiced.

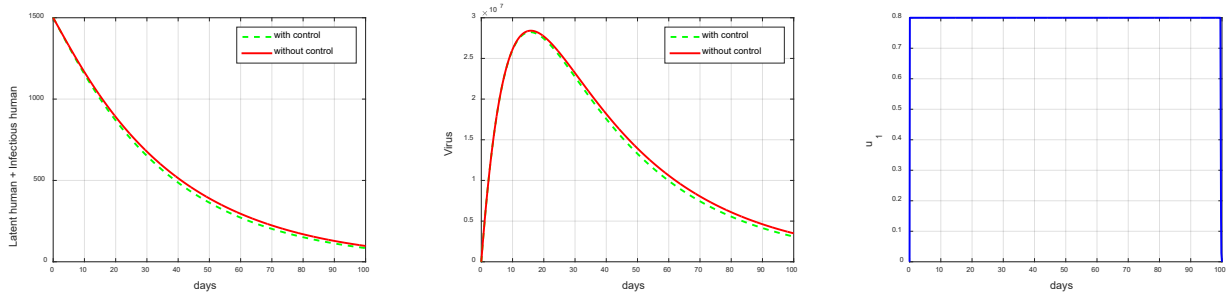

(a). $L(t)+I(t)$ **(b).** $V(t)$ **(c).** $u_1(t)$

Figure 5. Dynamics of infected humans, viruses, and control profile when strategy 1 is applied.

Strategy 2

To study the dynamics of the spread of covid-19 when only handwashing intervention is applied, we conduct numerical simulations. The dynamic of infected human and viruses can be seen in Figure 6(a) and 6(b). If strategy 2 is used with u_2 at its highest value during the simulation period as seen in Figure 6(c), the number of latent humans, infectious humans, and viruses at the end of the simulation are 5, 14, and 954453, respectively. It is clear that there is a significant decrease in the number of infected humans and viruses when strategy 2 is implemented. This is different from the results when strategy 1 is applied.

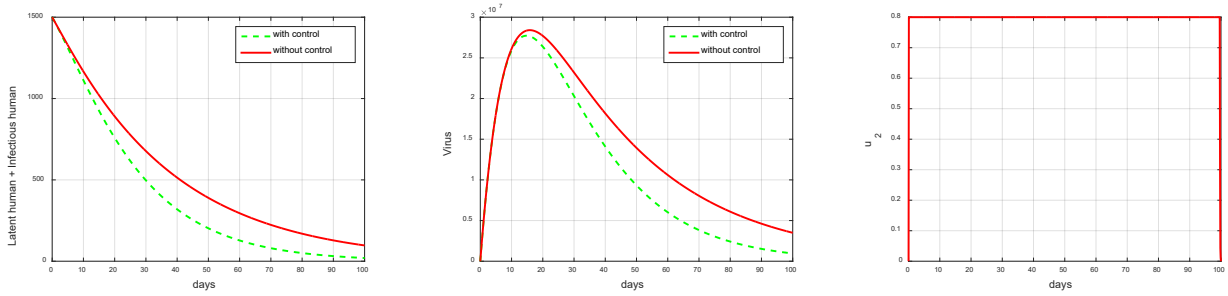

(a). $L(t)+I(t)$ **(b).** $V(t)$ **(c).** $u_2(t)$

Figure 6. Dynamics of infected humans, viruses, and control profile when strategy 2 is applied.

Strategy 3

The third simulation of optimal control problem is carried out to study the impact of implementing strategy 3 on the spread of covid-19. As we can observe in Figure 7(a), the dynamics of infected humans are similar to Figure 6(a). However, a significant difference is seen in the dynamics of the viruses as can be seen in Figure 7(b). The numerical simulation results show that the number of latent humans, infectious humans, and viruses on day 100 are 5, 14, 191095, respectively. It is clear that there is a very extreme decline in the number of viruses when compared to the number of viruses when strategy 1 or strategy 2 is involved. This happens because 80% of infected humans use masks during the simulation period as shown in figure 7(c).

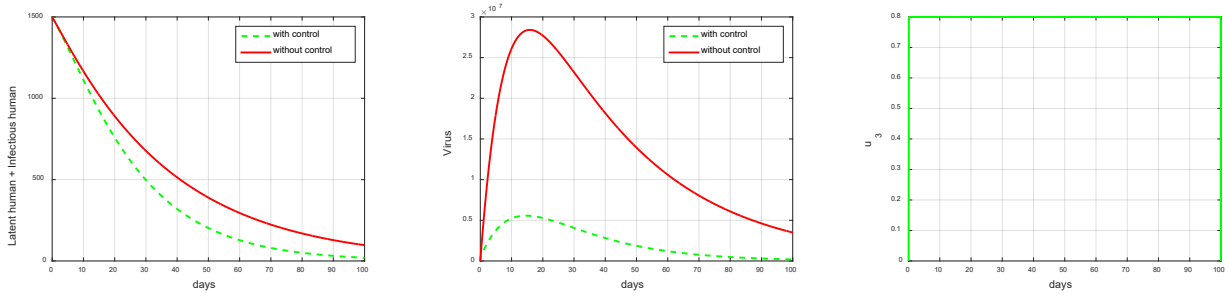

(a). $L(t)+I(t)$ **(b).** $V(t)$ **(c).** $u_3(t)$

Figure 7. Dynamics of infected humans, viruses, and control profile when strategy 3 is applied.

Strategy 4

Now we discuss the results of the numerical simulation of the optimal control problem when implementing strategy 4. It seems that the dynamics of infected humans and viruses as shown in Figures 8(a) and 8(b) are very similar to those of Figures 6(a) and 6(b). Nevertheless, the numerical solution shows the number of latent humans, infectious humans, and viruses at the end of the simulation course is 3, 11, and 782673, respectively. It is clear that the difference in the outcomes of implementing strategy 2 and strategy 4 is not significant even though u_1 and u_2 are at their maximum values during the simulation period as seen in Figure 8(c).

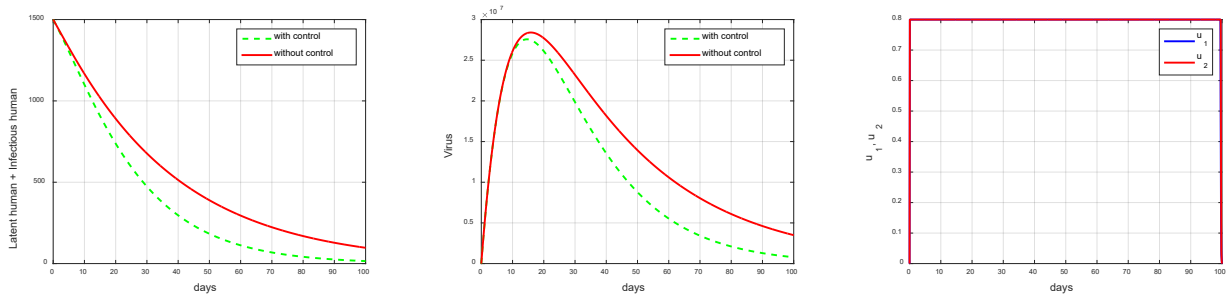

(a). $L(t)+I(t)$ **(b).** $V(t)$ **(c).** $u_1(t), u_2(t)$

Figure 8. Dynamics of infected humans, viruses, and control profile when strategy 4 is practiced.

Strategy 5

Figure 9 shows the results of the numerical simulation of the optimal control problem when the intervention employed is social distancing and handwashing. Notice that the dynamics of infected humans (Figure 9a) and viruses (Figure 9b) are very similar to the results of the third numerical simulation as shown in Figure 7. However, if strategy 5 is applied, the number of latent humans, infectious humans, and viruses on day 100 are 3, 11, and 156712, respectively. Obviously, the prevalence of covid-19 is smaller than when strategy 3 is applied. Figure 9(c) shows that we have to keep control u_3 at its maximum bound longer than u_1.

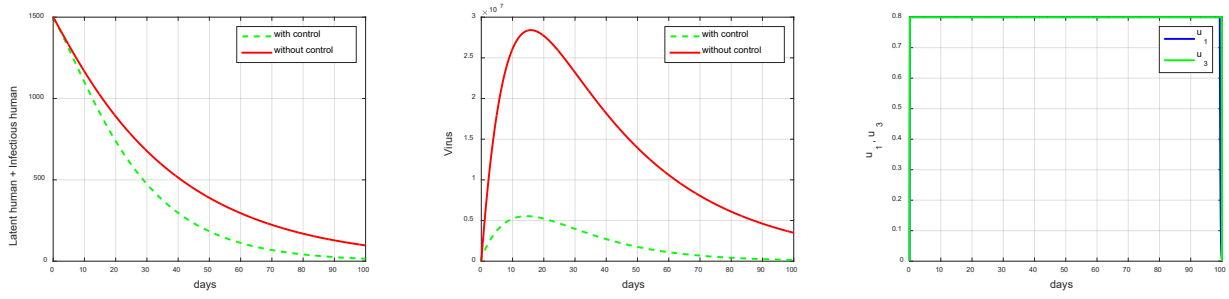

(a). $L(t)+I(t)$ **(b).** $V(t)$ **(c).** $u_1(t), u_3(t)$

Figure 9. Dynamics of infected humans, viruses, and control profile when strategy 5 is practiced.

Strategy 6

The sixth simulation is performed to see the impact of implementing strategy 6. As shown in Figures 10(a) and 10(b), the dynamics of the spread of covid-19 are very similar to those shown in Figures 9(a) and 9(b). If strategy 6 is applied, the number of latent humans, infected humans, and virus at day 100 are 2, 9, and 130252, respectively. It is clear that the number of infected humans and viruses when strategy 6 is applied is the smallest compared to the previous simulations. Figure 10(c) tells us that we should lower the control u_2 first than u_3.

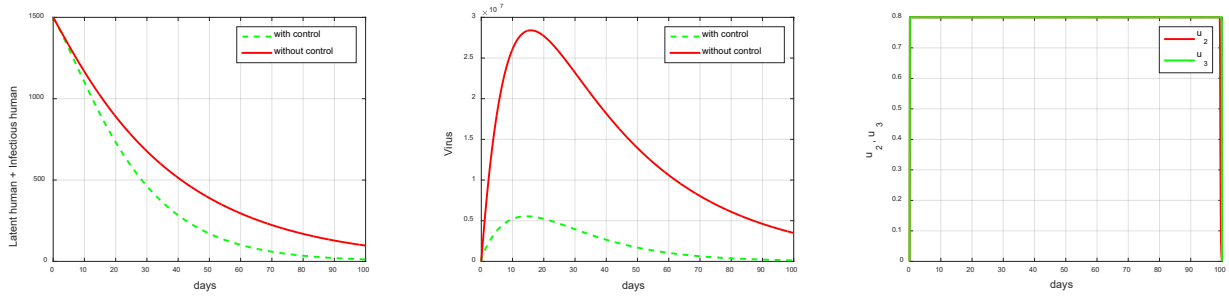

(a). $L(t)+I(t)$ **(b).** $V(t)$ **(c).** $u_2(t), u_3(t)$

Figure 10. Dynamicss of infected humans, viruses, and control profile when strategy 6 is practiced.

Strategy 7

The last simulation of the optimal control problem is carried out to examine the dynamics of the spread of covid-19 when strategy 7 is implemented. The dynamic of infected human and virus can be seen in Figure 11(a) and Figure 11(b),

respectively. The number of latent human, infectious human, and virus are 1, 7, and 102878, respectively. Figure 11(c) shows that we should keep cotrol u_3 at its maximum bound longer than u_1 and u_2. Clearly, strategy 7 provides the best results compared to other strategies when viewed from the prevalence of covid-19.

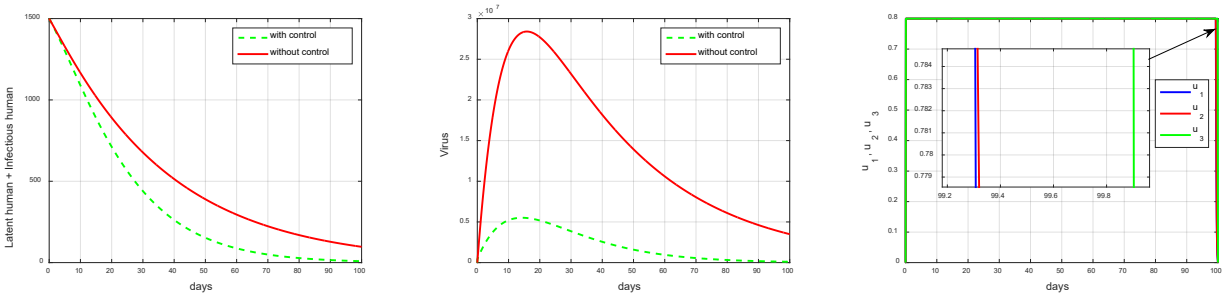

(a). $L(t)+I(t)$ **(b).** $V(t)$ **(c).** $u_1(t), u_2(t), u_3(t)$

Figure 11. Dynamics of infected humans, viruses, and control profile when strategy 7 is practiced.

Cost-effectiveness analysis

Table 2. ACER and Effectiveness of each strategy.

Strategy	ACER	$\bar{E}$
1	6.9972×10^{-6}	0.0314
2	2.1241×10^{-7}	0.2076
3	5.2684×10^{-8}	0.8397
4	1.1438×10^{-6}	0.2312
5	3.1291×10^{-7}	0.8444
6	1.0423×10^{-7}	0.8468
7	3.6212×10^{-7}	0.8512

Cost-effectiveness analysis is carried out by determining the ACER of each strategy using (5). In addition, we also determine the effectiveness of each strategy in reducing the infected humans by using (3). The results are given in the Table 2. Obviously, strategy 7 has the highest effectiveness, which is 0.8512. Based on Table 2, the most effective strategy in reducing the number of infected humans is strategy 7 followed by strategy 6. According to [25], the most cost-effective strategy is the strategy that has the smallest ACER. Therefore, we conclude that strategy 3 is the most cost-effective strategy followed by strategy 6.

CONCLUSION

In this paper, we propose covid-19 model considering non-pharmaceutical intervention and indirect transmission. The model has two equilibrium points. The existence and local stability condition of all equilibrium points are given and proved. Our results show that non-pharmaceutical approach can be used to control the covid-19 spread. Our results show that combination of social distancing, handwashing, and mask-wearing is the most effective strategy to control covid-19 spread. Based on the ACER values, the most cost-effective strategy is mask-wearing. Furthermore, global sensitivity analysis result shows that parameter related to mask-wearing is the most influential parameter on basic reproduction number compared to parameter related to social distancing and handwashing.

REFERENCES

[1] H. Harapan *et al.*, "Coronavirus disease 2019 (COVID-19): A literature review," J. Infect. Public Health, vol. 13, no. 5, pp. 667–673, 2020.

[2] A. Jafari-Sales, H. Khaneshpour, M. Pashazadeh, and R. Nasiri, "Coronavirus disease 2019 (COVID-19): review study," Jorjani Biomed. J., vol. 8, no. 1, pp. 4–10, 2020.

[3] H. Ouassou *et al.* "The pathogenesis of Coronavirus disease 2019 (covid-19): evaluation and prevention," J. Immunol. Res., vol. 2020, pp. 1–7, 2020.

[4] H.A. Rothan and S.N. Byrareddy, "The epidemiology and pathogenesis of coronavirus disease (COVID-19) outbreak," J. Autoimmun., vol. 109, p. 102433, 2020.

[5] A.O. Fadaka *et al.*, "Understanding the epidemiology, pathophysiology, diagnosis and management of SARS-CoV-2," J. Int. Med. Res., vol. 48, no. 8, p. 030006052094907, 2020.

[6] J. Leap, V. Villgran, and T. Cheema, "COVID-19," Crit. Care Nurs. Q., vol. 43, no. 4, pp. 338–342, 2020.

[7] S.W.X. Ong *et al.*, "air, surface environmental, and personal protective equipment contamination by severe acute respiratory syndrome coronavirus 2 (SARS-CoV-2) from a symptomatic patient," JAMA, vol. 323, no. 16, p. 1610, 2020.
[8] S. Wu, Y. Wang, X. Jin, J. Tian, J. Liu, and Y. Mao, "Environmental contamination by SARS-CoV-2 in a designated hospital for coronavirus disease 2019," Am. J. Infect. Control, vol. 48, no. 8, pp. 910–914, 2020.
[9] S.E. Eikenberry *et al.*, "To mask or not to mask: modeling the potential for face mask use by the general public to curtail the COVID-19 pandemic," Infect. Dis. Model., vol. 5, pp. 293–308, 2020.
[10] D. Aldila, "COVID-19 disease transmission model considering direct and indirect transmission," E3S Web Conf., vol. 202, p. 12008, 2020.
[11] D. Aldila, "Optimal control problem on COVID-19 disease transmission model considering medical mask, disinfectants and media campaign," E3S Web Conf., vol. 202, p. 12009, 2020.
[12] M. Zamir, Z. Shah, F. Nadeem, A. Memood, H. Alrabaiah, and P. Kumam, "non pharmaceutical interventions for optimal control of COVID-19," Comput. Methods Programs Biomed., vol. 196, p. 105642, 2020.
[13] M. Zamir, T. Abdeljawad, F. Nadeem, A. Wahid, and A. Yousef, "An optimal control analysis of a COVID-19 model," Alexandria Eng. J., vol. 60, no. 3, pp. 2875–2884, 2021.
[14] S. İğret Araz, "Analysis of a Covid-19 model: optimal control, stability and simulations," Alexandria Eng. J., vol. 60, no. 1, pp. 647–658, 2021.
[15] V. P. Bajiya, S. Bugalia, and J. P. Tripathi, "Mathematical modeling of COVID-19: impact of non-pharmaceutical interventions in India," Chaos An Interdiscip. J. Nonlinear Sci., vol. 30, no. 11, p. 113143, 2020.
[16] L. Lemecha Obsu and S. Feyissa Balcha, "Optimal control strategies for the transmission risk of COVID-19," J. Biol. Dyn., vol. 14, no. 1, pp. 590–607, 2020.
[17] A. Meiksin, "Dynamics of COVID-19 transmission including indirect transmission mechanisms: a mathematical analysis," Epidemiol. Infect., vol. 148, p. e257, 2020.
[18] T.A. Perkins and G. España, "Optimal Control of the COVID-19 pandemic with non-pharmaceutical interventions," Bull. Math. Biol., vol. 82, no. 9, p. 118, 2020.
[19] S. Marino, I.B. Hogue, C.J. Ray, and D.E. Kirschner, "A methodology for performing global uncertainty and sensitivity analysis in systems biology," J. Theor. Biol., vol. 254, no. 1, pp. 178–196, 2008.
[20] X. Yang, L. Chen, and J. Chen, "Permanence and positive periodic solution for the single-species nonautonomous delay diffusive models," Comput. Math. with Appl., vol. 32, no. 4, pp. 109–116, 1996.
[21] P. van den Driessche and J. Watmough, "Reproduction numbers and sub-threshold endemic equilibria for compartmental models of disease transmission," Math. Biosci., vol. 180, no. 1–2, pp. 29–48, 2002.
[22] Handbook of Mathematics for Engineers and Scientists, Chapman & Hall/CRC, 2007.
[23] A. Liénard and M. H. Chipart, "Sur le signe de la partie réelle des racines d'une équation algébrique," J. Math. Pures Appl, vol. 10, no. 6, pp. 291–346, 1914.
[24] C. Castillo-Chavez and B. Song, "Dynamical models of tuberculosis and their applications," Math. Biosci. Eng., vol. 1, no. 2, pp. 361–404, 2004.
[25] D. Darmawati, M. Musafira, D. Ekawati, W. Nur, M. Muhlis, and S. F. Azzahra, "Sensitivity, optimal control, and cost-effectiveness analysis of intervention strategies of filariasis," Jambura J. Math., vol. 4, no. 1, pp. 64–76, 2022.
[26] B. Buonomo and R. Della Marca, "Optimal bed net use for a dengue disease model with mosquito seasonal pattern," Math. Methods Appl. Sci., 2017.
[27] D. Aldila, "Analyzing the impact of the media campaign and rapid testing for COVID-19 as an optimal control problem in East Java, Indonesia," Chaos, Solitons & Fractals, vol. 141, p. 110364, 2020.
[28] R. Memarbashi and S. M. Mahmoudi, "A dynamic model for the COVID-19 with direct and indirect transmission pathways," Math. Methods Appl. Sci., vol. 44, no. 7, pp. 5873–5887, 2021.
[29] D. Aldila, "Cost-effectiveness and backward bifurcation analysis on COVID-19 transmission model considering direct and indirect transmission," Commun. Math. Biol. Neurosci., 2020.